第 48 卷 第 23 期/2021 年 12 月/中国激光 研究论文

中国激光

噪声光注入分布式布拉格反射型激光器的混沌动力学特性

郭亘立[1,2]，贾志伟[1,2]，王安帮[1,2*]，王云才[3,4]

[1]太原理工大学新型传感器与智能控制教育部重点实验室，山西 太原 030024；

[2]太原理工大学物理与光电工程学院，山西 太原 030024；

[3]广东工业大学信息工程学院，广东 广州 510006；

[4]广东工业大学广东省光子学信息技术重点实验室，广东 广州 510006

摘要 研究了由噪声光驱动的分布式布拉格反射型(DBR)激光器的混沌动力学特性，观察到在边模注入时 DBR 激光器产生的混沌。研究了注入强度与频率失谐对混沌带宽和关联维度的影响。结果表明，噪声光在光谱边模注入时，DBR 激光器也可产生混沌，且混沌信号的低频频谱平坦。其关联维度的平均值为 1.86，维度的波动为±0.36，且混沌信号受注入噪声光的影响程度低。

关键词 激光器；半导体激光器；分布式布拉格反射器激光器；非线性动力学；混沌；光注入

中图分类号 TN248.4 **文献标志码** A **doi**：10.3788/CJL202148.2301003

1 引 言

混沌激光因其宽带和随机的特性而具有许多应用[1-3]。由噪声光驱动混沌同步的密钥分发方案因其具有高速潜力[4-6]、来自经典物理层的安全性及与现行光纤网络兼容等优点而备受关注。2012 年，日本的 Yoshimura 等[7]在实验中验证了基于噪声光注入带有光反馈的分布式反馈(DFB)激光器的混沌密钥分发方案[8-11]。2017 年，电子科技大学的 Jiang 等[12]在数值模拟上提出了基于垂直腔面发射激光器(VCSEL)双偏振模式的混沌密钥分发方案。2020 年太原理工大学的 Gao 等[13]实验上实现了基于噪声光共驱同步的法布里-珀罗(FP)激光器模式键控的混沌密钥分发方案。在上述方案中，为实现混沌密钥分发，需要外部调制器对混沌的相位、偏振或强度状态进行键控，从而实现键控混沌同步。但是外部调制器件的引入提高了系统的复杂度，不利于密钥分发系统的构建。

DBR 激光器[14-15]是一种波长可调谐的半导体激光器，通过调节加载在 DBR 区的电流可实现激光器输出波长的改变，进而实现 DBR 激光器混沌密钥分发系统中的波长键控。所以，研究噪声光注入 DBR 激光器的混沌动力学特性具有重要意义。

研究了 DBR 激光器在噪声光注入下的混沌动力学特性，当噪声光在主模注入时，DBR 激光器混沌动力学特性与 DFB 激光器类似；当噪声光与主模有较大频率失谐时，DBR 激光器表现出一种完全不同的混沌状态，此时其能量主要集中在频谱低频段。进一步研究了不同的频率失谐与注入强度下，DBR 激光器产生混沌激光的带宽和关联维。本研究工作为发展基于噪声光注入共驱 DBR 激光器同步的密钥分发技术提供了研究基础，也为边模噪声光注入下的混沌激光产生提供新的技术思路。

2 实验研究方案

实验装置如图 1(a)所示，由超辐射发光二极管

收稿日期：2021-04-19；**修回日期**：2021-05-05；**录用日期**：2021-05-12

基金项目：国家自然科学基金(61822509，61731014，61927811，61961136002)、山西省优秀人才科技创新项目(201805D211027)

通信作者：*wanganbang@tyut.edu.cn

(SLD)作为噪声光源，所发出的宽带噪声光经由隔离器(OI)单向注入可调谐光滤波器(TF_1，EXFO XTM-50)，将宽带噪声光滤波为所需的中心波长和光谱带宽，滤波后的光信号进入掺铒光纤放大器(EDFA，EOPSYS CEFA-C-HG)，对滤波后的噪声光信号进行功率放大，再经过可调谐光滤波器(TF_2，Yenista XTM-50)消除由 EDFA 引入的带外噪声，得到实验所需的噪声光。噪声光经可调光衰减器(VOA)、OI、3dB 耦合器(OC)和偏振控制器(PC)注入 DBR 激光器(PL-DBR-1550-30-1-SA-14BF-WOI)。VOA 用于调节注入光的光功率，OI 用于避免 DBR 激光器发射的激光对噪声光信号产生干扰，OC 用于将噪声光耦合进入 DBR 激光器，同时将 DBR 激光器发射激光耦合输出至另一光路，PC 用于控制注入噪声光的偏振状态。DBR 激光器是由增益区、相位区和 DBR 区组成三段式激光器，其阈值电流 I_{th} 为 43.2 mA，功率斜效率为 0.205 mW/mA，中心波长可在 1545.2～1553.7 nm 之间调谐，以及约 45 GHz 的自由光谱范围。DBR 激光器发射激光经由 PC 和 OC 耦合输出至 EDFA(EDFA-DCB-25-1-FC / APC)进行功率放大，以便于之后对的光探测，放大的光信号通过可调谐滤波器(TF_3，EXFO XTM-50)只滤出 DBR 激光器的激射波长，从而排除噪声光对于测试结果的干扰。然后，光信号被两个 OC 分成三路进行分别检测。光信号的光谱由光谱分析仪(YOKOGAWA AQ6370D 0.02 nm 分辨率)进行测量，时域波形和功率谱由 40 GHz 光电探测器(Finisar XPDV2120RA)转换为电信号后，由宽带示波器(LeCroy LABMASTER10ZI，36 GHz 带宽)和频谱分析仪(Rohde&Schwarz FSW50，50 GHz 带宽)进行测量。

图 1(b)为自由运行的 DBR 激光器的光谱(虚线)和经由滤波、放大、再滤波后的噪声光光谱(实线)。在整个实验过程中，DBR 激光器的增益区电流设置为 57.6 mA(1.33I_{th})，DBR 区电流为 12.1 mA，激光器输出的波长 $\lambda_{SLD}=c/\upsilon_{DBR}$ 为 1549.2540 nm，υ_{DBR} 为激光波长对应的频率，c 为真空光速，激光器输出光功率 P_{DBR} 为 1.85 mW；SLD(Thorlabs 1005S)偏置电流为 350.0 mA，发射光全谱总功率为 12.42 mW，TF_1 和 TF_2 都具有 6 GHz 的 3dB 滤波线宽和相同的中心波长 λ_{SLD}(频率 υ_{SLD})。另外，可调谐滤波器 TF_3 的滤波线宽和中心波长随 DBR 激光器发射混沌激光的状态进行调整，以确保可滤出整个混沌信号，并且保证探测信号不受注入噪声光的干扰。

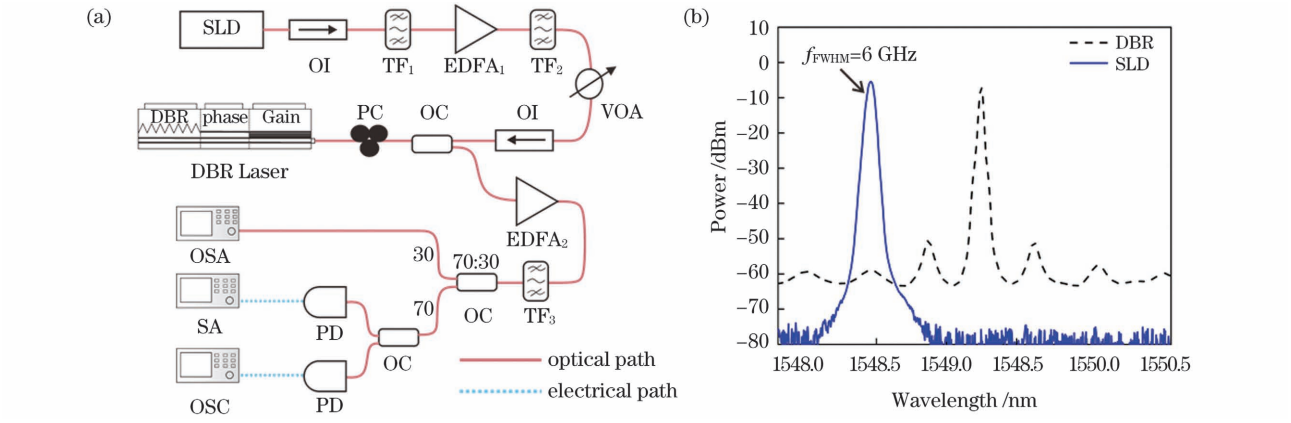

图 1　实验原理图。(a)实验装置；(b)光谱

Fig. 1　Experimental schematic. (a) Experimental setup; (b) optical spectrum

3　实验结果及分析

3.1　实验结果

图 2 展示了噪声光滤波前后的光谱、频谱与时域波形。图 2(a)为未经滤波的光谱，其在输出光谱范围内几乎为一条直线，其频谱与基底噪声相似，具有宽带特性，如图 2(b)所示。图 2(c)为噪声信号的时域波形。图 2(d)为滤波后具有 6 GHz 的 3 dB 线宽的高斯形噪声光谱。其频谱如图 2(e)所示，类似为经过低通滤波器的噪声频谱。图 2(f)展示的时域波形表现为噪声的随机起伏。在噪声光注入激光器产生混沌的密钥分发系统中，外部噪声光子消耗了激光器内的载流子使得响应激光器进入混沌状态，且驱动噪声信号与响应混沌信号几乎没有相关性，这使得窃听者不能在公共信道中提取与密钥相关的信息，提高了系统的安全性[10-11]。

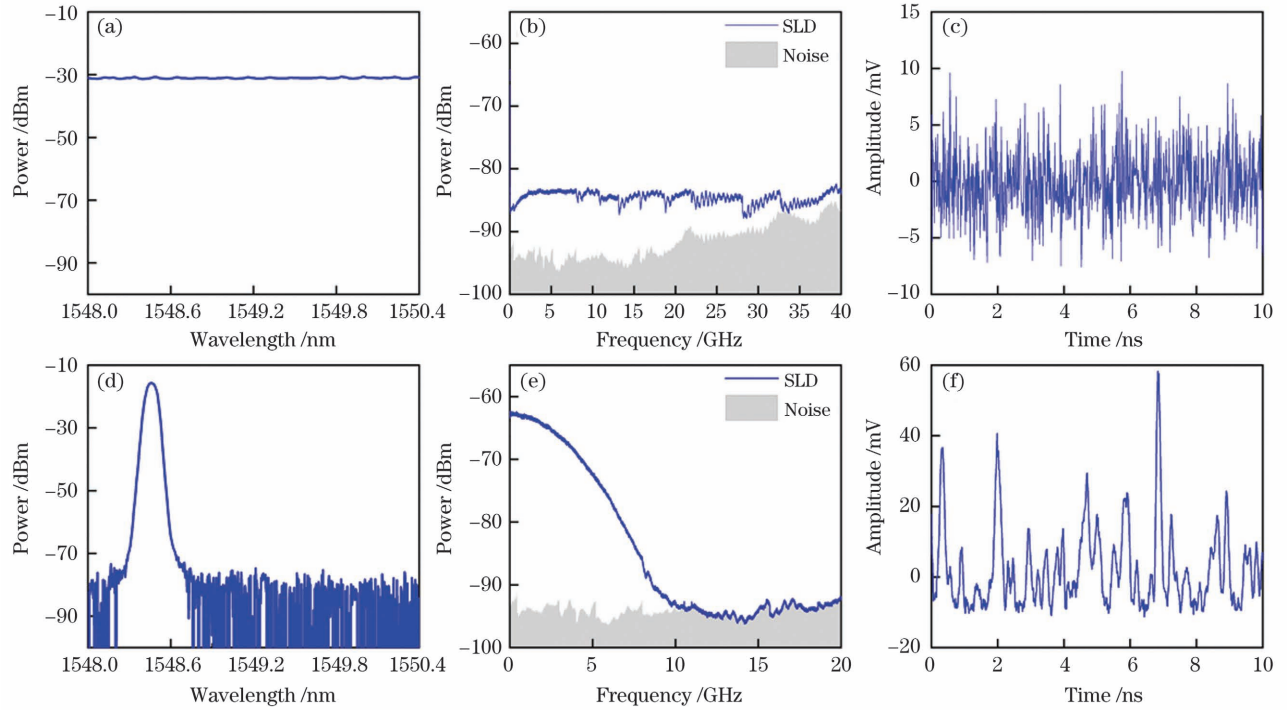

图 2 噪声光滤波前后的特性。(a)(d)噪声光滤波前后的光谱;(b)(e)噪声光滤波前后的频谱;(c)(f)噪声光滤波前后的时域波形

Fig. 2 Characteristics of noise light before and after filtering. (a)(d) Spectrums of noise light before and after filtering; (b)(e) frequency spectraof noise light before and after filtering; (c)(f) temporal waveforms of noise light before and after filtering

图 3 为不同频率失谐 $\Delta v = v_{DBR} - v_{SLD}$ 下 DBR 激光器产生混沌的光谱、频谱和时域波形图。测试过程中固定噪声光注入强度 $\kappa_j = (P_{SLD}/P_{DBR})$ 为 0.32，P_{SLD} 为进入 DBR 激光器的噪声光功率。光谱图中的点划线和实线分别是噪声光注入下 DBR 激光器的未经 $EDFA_2$ 放大与 TF_3 滤波的光谱，和经过 $EDFA_2$ 放大与 TF_3 滤波之后的光谱。

当 $\Delta v = 0$ 时，即主模噪声光注入下，激光输出为典型的混沌激光状态，80% 能量带宽为 7.3 GHz[16]，混沌起伏幅值较大，约 −20～80 mV。此时，混沌激光特性与光注入普通 DFB 激光器所产生的混沌激光特性相似。

当 Δv 的增大至 1/2 激光器腔模间隔时，激光器输出为一种不同的混沌激光状态，其能量主要集中在低频段。进一步增大 Δv，当注入噪声光的中心波长位于 DBR 激光器两个模式之间的谷值，如图 3(b1)(b2)(b3)和(d1)(d2)(d3)，对应的 Δv 分别为 27.5 GHz 和 81.5 GHz，混沌激光频谱成“倒对勾”状，弛豫振荡峰明显，其 80%能量带宽分别为 1.36 GHz 和 1.29 GHz，时序表现为明显的混沌振荡状态但幅值波动较小。当注入噪声光的中心波长位于 DBR 光谱边模的峰值处，如图 3(c1)(c2)(c3)与(e1)(e2)(e3)，对应的 Δv 分别为 47.5 GHz 和 104.5 GHz，混沌激光频谱在低频段平坦，弛豫振荡峰几乎消失，其 80%能量带宽分别为 1.10 GHz 和 1.07 GHz，时域波形的幅值波动强于注入噪声光处于模式间谷值的情况，其波形为类脉冲状。

在光注入 DFB 激光器中，产生混沌激光要求注入光与激光器主模具有小的频率失谐，当注入光波长处于边模处时，无法产生混沌激光[17]。在注入光与激光器主模频率失谐大于激光器腔模间隔情况下，甚至频率失谐高达 104.5 GHz 时，DBR 激光器仍能产生混沌激光的现象。其原因是，在 DBR 激光器中，由于 DBR 反射带中包含有多个腔模，主模与边模的模式竞争更强。实验所用 DBR 激光器在自由输出时，其边模抑制比为 43.37 dB，当在模式间隔调节 DBR 区电流时，激光器甚至会出现双模输出现象。当外部注入光处于边模注入状态时，进一步增强主模与边模的模式竞争，从而使主模和边模一起进入混沌振荡状态。DFB 激光器中边模强度远小于主模，其边模抑制比一般大于 50 dB，边模光注入下，边模状态的变化无法影响主模。

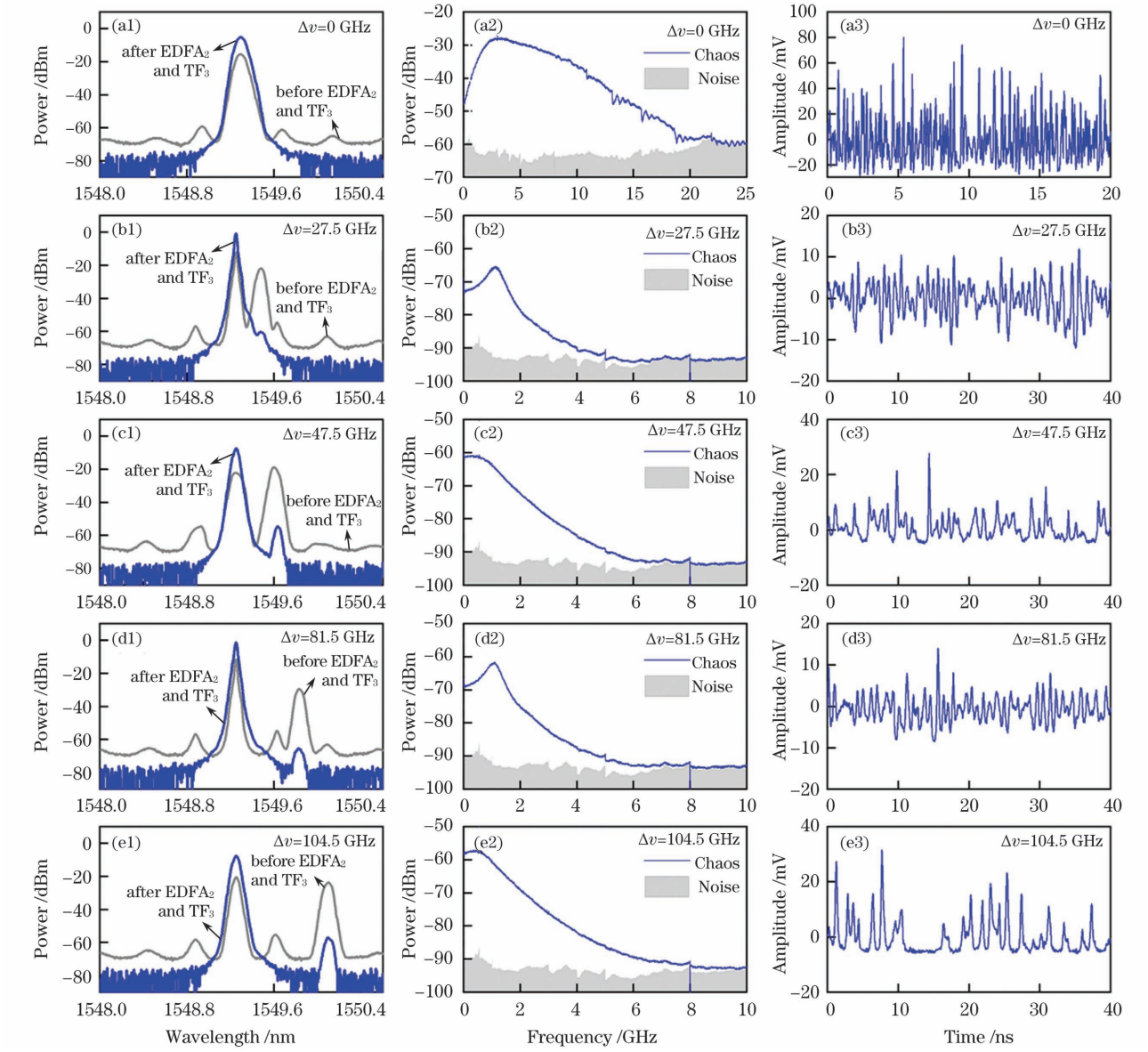

图 3 不同频率失谐下 DBR 激光器产生混沌的光谱、频谱和时域波形图。(a1)(b1)(c1)(d1)(e1)不同频率失谐下 DBR 激光器产生混沌的光谱图；(a2)(b2)(c2)(d2)(e2)不同频率失谐下 DBR 激光器产生混沌的频谱图；(a3)(b3)(c3)(d3)(e3)不同频率失谐下 DBR 激光器产生混沌的时域波形图

Fig. 3 Spectral, frequency spectral, time-domain of chaos in DBR laser under different frequency detunings. (a1)(b1)(c1)(d1)(e1) Spectral of chaos in DBR laser under different frequency detunings; (a2)(b2)(c2)(d2)(e2) frequency spectraof chaos in DBR laser under different frequency detunings; (a3)(b3)(c3)(d3)(e3) temporal waveforms of chaos in DBR laser under different frequency detunings

3.2 注入强度对混沌带宽的影响

图 4 为注入强度对混沌带宽的影响。如图 4(a)所示，当注入光在主模($\Delta v=0$ GHz)时，由 DBR 激光器产生的信号带宽随注入强度的增加而增加。可以看出，当 $\kappa_j>0.03$ 时，混沌带宽随注入强度的增加而迅速增加。最后，当 $\kappa_j>0.2$ 时激光器的带宽不再显著增加。注入光的中心波长移动到边模($\Delta v=104.5$ GHz)，观察注入强度对 DBR 激光器产生的混沌带宽的影响，如图 4(b)，带宽随注入强度的增加而减小。这是因为随着注入强度的增加，混沌频谱的弛豫振荡频率降低。并且低频能量增加使得频谱变得平坦，在 DC 至 80% 能量带宽的计算方法下，带宽随着注入强度的增加而减小。

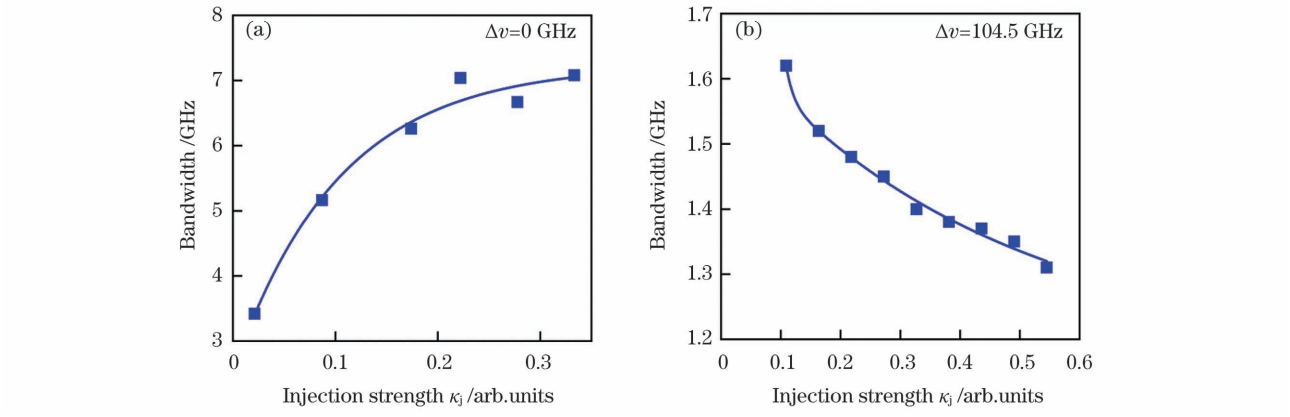

图 4　注入强度对混沌带宽的影响

Fig. 4　Effect of injection strength on chaotic bandwidth

3.3　频率失谐与注入强度对混沌关联维度的影响

关联维度是表征混沌时间序列的重要参数，它反映了系统的复杂度，用 G-P 算法计算了由 DBR 激光器产生的混沌时域波形的关联维度[18]。每次计算含 20000 个时域波形点，并在不同时间段为每组时域波形计算 10 次。图 5 为关联维度的结果图，图中的圆点是 10 次结果的平均值，误差棒为 3 倍的标准偏差。如图 5(a)为在不同频率失谐下注入强度 κ_j 固定为 0.32 时的关联维度。当注入光在主模($\Delta v=0$ GHz)时，混沌的关联维度最大，其平均值为 6.17。此时的混沌是高维混沌，关联维度的波动也是最明显的，其值为±2.02。在其他边模注入情况下，关联维度的平均值约为 1.86，并且波动在±0.36。当注入的噪声光和 DBR 激光器的频率失谐较小时，系统的复杂度较高，并且系统的复杂度大幅波动。这是因为当频率失谐较小时，外部注入光的光子频率更接近激光激射模式所消耗载流子的频率，产生的混沌现象更加明显，因此关联维度更大。图 5(b)为当主模($\Delta v=0$ GHz)时，混沌的关联维度随注入强度的增加而变化的趋势。曲线是平均值的拟合。当 $\kappa_j<0.18$ 时，混沌的关联维度的平均值显著增加，而当 $\kappa_j>0.18$ 时，维度的均值增加趋于稳定，稳定在 6.1 左右。注入强度对关联维度的波动没有影响，波动主要来自于噪声光驱动下的混沌本身。

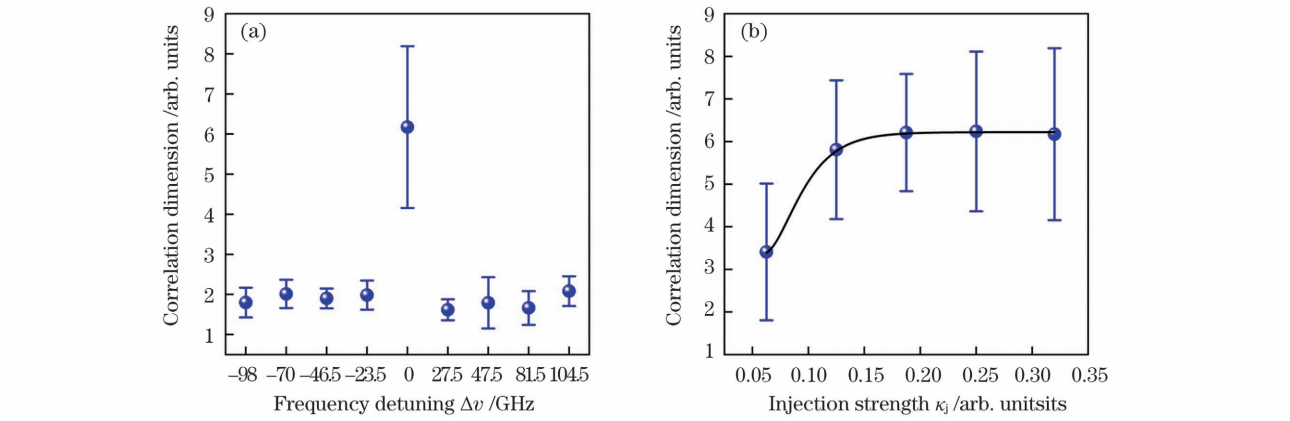

图 5　注入光参数对关联维度的影响。(a)频率失谐；(b)注入强度

Fig. 5　Effect of injected light parameters on correlation dimension. (a) Frequency detuning; (b) injection strength

噪声光驱动的密钥分发系统下，噪声光信号会不可避免的被引入探测端，探测过程中引入噪声光会降低合法用户的同步系数，从而增大密钥误码率。这种现象不利于混沌密钥分发。在边模注入的情况下，滤波器可以避免引入噪声光，混沌关联维度和维度的波动较小，易于获得更高的同步系数，有利于密钥分发。

4　结　　论

面向混沌密钥分发应用需求，本文在实验上研究噪声光注入 DBR 激光器的混沌动力学特性。研究表明，当噪声光处于主模注入区间时，DBR 激光器表现出与光注入 DFB 激光器相似的混沌状态；当噪声光处于边模注入区间时，DBR 激光器表现出另

一种混沌状态，其能量主要集中于低频段，弛豫振荡峰不明显。进一步研究了不同频率失谐、注入强度下，混沌激光的带宽和关联维度。发现在边模注入下，关联维度的波动小，并且在探测过程中引入的噪声分量较低，这更有利于构造混沌密钥分发系统。

参 考 文 献

[1] Sun W Y, Hu B J, Wang H. Chaos synchronization communication based on dual-path mutual coupling semiconductor lasers[J]. Laser & Optoelectronics Progress, 2019, 56(21): 211404.
孙巍阳, 胡宝洁, 王航. 双光互注入半导体激光器混沌同步通信研究[J]. 激光与光电子学进展, 2019, 56(21): 211404.

[2] Hu Z H, Zhao T, He P X, et al. Improving dynamic range of chaos optical time domain reflectometry using fiber ring[J]. Chinese Journal of Lasers, 2019, 46(10): 1004006.
胡志宏, 赵彤, 贺培鑫, 等. 基于光纤环的混沌光时域反射仪动态范围增大[J]. 中国激光, 2019, 46(10): 1004006.

[3] Yan S L. Theory and technique of cross transmittance and alternate parallel reception of laser chaos in secure communication[J]. Chinese Journal of Lasers, 2020, 47(9): 0906001.
颜森林. 激光混沌交叉发射与交替并行接收在保密通信中应用的基本理论与技术[J]. 中国激光, 2020, 47(9): 0906001.

[4] Uchida A, Amano K, Inoue M, et al. Fast physical random bit generation with chaotic semiconductor lasers[J]. Nature Photonics, 2008, 2(12): 728-732.

[5] Wang A B, Wang L S, Li P, et al. Minimal-post-processing 320-Gbps true random bit generation using physical white chaos[J]. Optics Express, 2017, 25(4): 3153-3164.

[6] Li P, Wang Y C. Research progress in physical random number generator based on laser chaos for high-speed secure communication [J]. Laser & Optoelectronics Progress, 2014, 51(6): 060002.
李璞, 王云才. 面向高速保密通信的激光混沌物理随机数发生器研究进展[J]. 激光与光电子学进展, 2014, 51(6): 060002.

[7] Yoshimura K, Muramatsu J, Davis P, et al. Secure key distribution using correlated randomness in lasers driven by common random light[J]. Physical Review Letters, 2012, 108(7): 070602.

[8] Koizumi H, Morikatsu S, Aida H, et al. Information-theoretic secure key distribution based on common random-signal induced synchronization in unidirectionally-coupled cascades of semiconductor lasers[J]. Optics Express, 2013, 21(15): 17869-17893.

[9] Sasaki T, Kakesu I, Mitsui Y, et al. Common-signal-induced synchronization in photonic integrated circuits and its application to secure key distribution [J]. Optics Express, 2017, 25(21): 26029-26044.

[10] Suzuki N, Hida T, Tomiyama M, et al. Common-signal-induced synchronization in semiconductor lasers with broadband optical noise signal[J]. IEEE Journal of Selected Topics in Quantum Electronics, 2017, 23(6): 1-10.

[11] Tomiyama M, Yamasaki K, Arai K, et al. Effect of bandwidth limitation of optical noise injection on common-signal-induced synchronization in multi-mode semiconductor lasers [J]. Optics Express, 2018, 26(10): 13521-13535.

[12] Jiang N, Xue C P, Liu D, et al. Secure key distribution based on chaos synchronization of VCSELs subject to symmetric random-polarization optical injection[J]. Optics Letters, 2017, 42(6): 1055-1058.

[13] Gao H, Wang A B, Wang L S, et al. High-speed physical key distribution based on mode-keying chaos synchronization of Fabry-Perot lasers [EB/OL]. (2020-04-18)[2021-04-15]. https://arxiv.org/abs/2004.08586.

[14] Buus J, Murphy E J. Tunable lasers in optical networks [J]. Journal of Lightwave Technology, 2006, 24(1): 5-11.

[15] Zhou D B, Lu D, Liang S, et al. Transmission of 20 Gb/s PAM-4 signal over 20 km optical fiber using a directly modulated tunable DBR laser[J]. Chinese Optics Letters, 2018, 16(9): 091401.

[16] Lin F Y, Liu J M. Nonlinear dynamical characteristics of an optically injected semiconductor laser subject to optoelectronic feedback[J]. Optics Communications, 2003, 221(1/2/3): 173-180.

[17] Hwang S K, Liu J M. Dynamical characteristics of an optically injected semiconductor laser[J]. Optics Communications, 2000, 183(1/2/3/4): 195-205.

[18] Grassberger P, Procaccia I. Measuring the strangeness of strange attractors [J]. Physica D: Nonlinear Phenomena, 1983, 9(1/2): 189-208.

Chaotic Dynamics in DBR Laser with Noise-light Injection

Guo Genli [1,2], Jia Zhiwei [1,2], Wang Anbang [1,2*], Wang Yuncai [3,4]

[1] *Key Laboratory of Advanced Transducers and Intelligent Control System, Ministry of Education, Taiyuan University of Technology, Taiyuan, Shanxi* 030024, *China*;

[2] *College of Physics and Optoelectronics, Taiyuan University of Technology, Taiyuan, Shanxi* 030024, *China*;

[3] *School of Information Engineering, Guangdong University of Technology, Guangzhou, Guangdong* 510006, *China*;

[4] *Guangdong Provincial Key Laboratory of Photonics Information Technology, Guangdong University of Technology, Guangzhou, Guangdong* 510006, *China*

Abstract

Objective Chaos synchronisation key distribution driven by a common noise light has higher security because the synchronisation coefficient between the driven signal and the response signal is low, and the eavesdropper cannot restore the complete drive signal and extract the key information from the drive signal, which is essential. Distributed feedback (DFB) laser, a vertical cavity surface-emitting laser and Fabry-Perot laser chaos key distribution systems driven by noise light have all been reported. To realise the chaos key distribution in the above-mentioned scheme, the synchronisation of the chaos and external modulator must modulate the phase polarisation or intensity state of chaos, which increases the complexity of the system, Meanwhile, it is not conducive to the construction of the key distribution system. The distributed Bragg reflector (DBR) laser is a semiconductor laser with a tunable wavelength. The laser output wavelength can be changed by adjusting the current loaded in the DBR region, and then the wavelength input in the chaotic secret distribution system of the DBR laser can be realised. Therefore, it is significance to study the chaotic dynamic characteristics of noise light injected into DBR lasers. In this paper, the chaotic dynamic characteristics of the DBR laser under the injection of noise light are experimentally studied. We found that when the noise light has a large frequency detuning with the main mode, the DBR laser exhibits a completely different chaotic state and its energy is mainly concentrated in the low-frequency range. This paper provides a foundation for high-speed key distribution technology using the synchronisation of noise-light injection common-drive DBR lasers.

Methods The noise light generated by the super-luminescent diode (SLD) is filtered, amplified and refiltered by a tunable filter (TF_1), erbium-doped fibre amplifier ($EDFA_1$) and TF_2 before the injection of noise light in DBR laser. The optical path uses a variable optical attenuator and polarisation controller to adjust the optical power and polarisation of the injected light. The chaotic signal of the DBR laser is amplified and filtered by $EDFA_2$ and TF_3, respectively. It is divided into three paths of detection by two optical couplers. In the experiment, the DBR laser gain region current is set to 57.6 mA (1.33 I_{th}), the DBR region current is 12.1 mA, the free-running centre wavelength of the laser output is 1549.2540 nm (frequency v_{DBR}) and the optical power (P_{DBR}) is 1.85 mw. Furthermore, the bias current of SLD is 350.0 mA, while the total power of the emitted light is 12.42 mW. Both TF_1 and TF_2 have a 3-dB filter linewidth of 6 GHz and the same centre wavelength with λ_{SLD} (frequency v_{SLD}). Additionally, the filter line width and centre wavelength of the tunable filter TF_3 are adjusted according to the state of the chaotic laser emitted by the DBR laser to ensure that the entire chaotic signal can be filtered out and the interference of the detection signal on the injected noise light (Fig. 1).

Results and Discussions The optical spectra; electrical spectra and temporal waveforms of the injected light show the injected light is a noise signal (Fig. 2). We fix noise-light injection strength $\kappa_i = (P_{SLD}/P_{DBR}) = 0.32$, where P_{SLD} is the noise-light power entering the DBR laser. When $\Delta v = v_{DBR} - v_{SLD}$ is 0 GHz, that is, under the main mode noise-light injection, the laser output is like those produced by light injection into ordinary DFB lasers. Further increase of Δv when the centre wavelength of the injected noise light is in the valley between the two modes of the DBR laser, their corresponding Δv are 27.5 GHz and 81.5 GHz, respectively. At this time, the chaotic electrical spectra are inverted "check" shape, the relaxation oscillation peak are obvious, and their 80% energy bandwidth are 1.36 GHz and 1.29 GHz. The temporal waveforms show an obvious chaotic oscillation state, but the amplitude fluctuation is small. When the centre wavelength of the injected noise light is at the peak of the DBR optical spectrum side mode, the Δv values are 47.5 GHz and 104.5 GHz. The chaotic laser electrical spectra are flat in the low-

frequency band, and the oscillation peaks are almost disappeared, and their 80% energy bandwidth are 1.10 GHz and 1.07 GHz (Fig. 3). Furthermore, when the noise light is at the main mode, the chaotic bandwidth decreases as the injection strength decreases. When noise light is at the side mode, the chaotic bandwidth decreases as the injection strength increases (Fig. 4). Moreover, the correlation dimension of chaos reflects the complexity of the system. When the noise light is injected into the main mode, the correlation dimension of the chaos generated by the DBR laser is 6.17 ± 2.02; and when the side mode is injected, it is 1.86 ± 0.36. Meanwhile, when the noise light is in the main mode, the injection strength has little effect on the fluctuation of the correlation dimension, which shows that the chaotic complexity is higher, and the fluctuation comes from chaos itself and has little relation with external noise (Fig. 5). In key distribution system driven by noise light, the driven signal will inevitably be introduced into the detection end. This process will reduce the synchronisation coefficient of the legitimate user, and the phenomenon is not conducive to the chaos key distribution. In the case of side mode injection, the filter can avoid the introduction of noise light. Additionally, the chaos correlation dimension and the fluctuation of the dimension are small. It is easy to obtain a higher synchronisation coefficient, which is conducive to chaos synchronisation key distribution.

Conclusions Facing the application requirements of chaos key distribution, this paper experimentally studies the chaotic dynamics characteristics of noise light injected into DBR lasers. The study found that when noise light is in the main mode injection interval, the DBR laser shows a chaotic state similar to that of the light-injected DFB laser. When the noise light is in the side mode injection interval, the DBR laser shows a different chaotic state. It is mainly concentrated in the low-frequency band, and the relaxation oscillation peak is not obvious. We further studied the bandwidth and correlation dimension of chaotic lasers under different frequency detuning and injection strength and found that underside mode injection the correlation dimension is 1.86 ± 0.36, the noise component introduced in the detection process is low, which is more conducive to the construction of chaos key distribution system.

Key words lasers; semiconductor laser; distributed Bragg reflector laser; nonlinear dynamics; chaos

OCIS codes 140.5960; 140.3600; 190.3100; 140.1540